IEEE Photonics Journal
An IEEE Photonics Society Publication

Photon Counting Integral Imaging Using Compound Photon Counting Model and Adaptive Parametric Maximum Likelihood Estimator

Volume 9, Number 6, December 2017

Jiajia Qi
Guohua Gu
Weiji He
Qian Chen

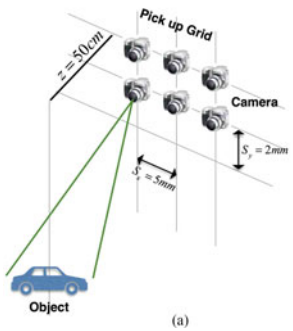

(a)

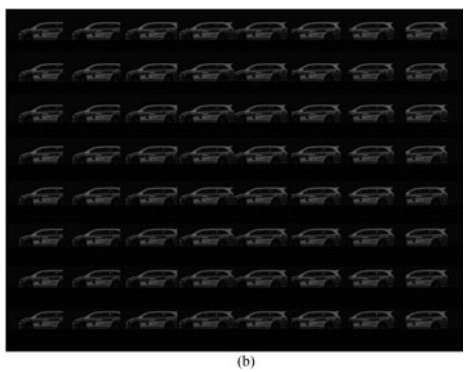

(b)

DOI: 10.1109/JPHOT.2017.2761181
1943-0655 © 2017 IEEE

Photon Counting Integral Imaging Using Compound Photon Counting Model and Adaptive Parametric Maximum Likelihood Estimator

Jiajia Qi,[1] Guohua Gu,[1] Weiji He,[1,2] and Qian Chen[1]

[1] Jiangsu Key of Spectral Imaging and Intelligence Sense, Nanjing University of Science and Technology, Nanjing 210094, China
[2] Key Laboratory of Intelligent Perception and Systems for High-Dimensional Information of the Ministry of Education, Nanjing University of Science and Technology, Nanjing 210094, China

DOI:10.1109/JPHOT.2017.2761181

Manuscript received August 14, 2017; revised October 3, 2017; accepted October 5, 2017. Date of current version October 27, 2017. This work was supported in part by the Seventh Six-talent Peak project of Jiangsu Province under Grant 2014-DZXX-007, in part by the National Natural Science Foundation of China under Grant 61271332, in part by the Fundamental Research Funds for the Central Universities under Grant 30920140112012, in part by the Innovation Fund Project for Key Laboratory of Intelligent Perception and Systems for High-Dimensional Information of Ministry of Education under Grant JYB201509, and in part by the Fund Project for Low-light-level Night Vision Laboratory under Grant J20130501. Corresponding author: Guohua Gu (e-mail: gghnjust@mail.njust.edu.cn).

Abstract: In this paper, a statistical approach based on an adaptive parametric estimator is proposed for the three-dimensional (3-D) reconstruction of objects under photon-starved conditions. In photon counting integral imaging system, 3-D objects having small number of photons can be visualized by the prior-based statistical estimation. However, improper prior constrains can lead to inaccurate reconstruction results. The adaptive parametric Maximum likelihood estimator (MLE) using a compound photon counting model is proposed to visualize the photon-limited 3-D objects. Through maximizing a likelihood function with pixel-based adaptive information, the number of photons for reconstructed pixels is estimated. Variance stabilizing transformation combined with Block-matching and 3-D filtering algorithm is also applied to enhance the photon counting elemental images captured by the photon counting integral imaging system. The performance of our proposed reconstruction method is illustrated by experimental results and compared with conventional MLE using the peak signal-to-noise ratio metric. It is shown that our proposed method outperforms the conventional MLE for the photon counting 3-D integral imaging reconstruction.

Index Terms: Photon counting, integral imaging, variance stabilizing transformation combined with block-matching and three dimensional (3-D) filtering (VST+BM3D), 3-D reconstruction.

1. Introduction

Different from traditional imaging devices requiring a large photon flux, a photon counting detector can capture significant information through very few photons per pixel. Based on the Poisson distribution modeling photon events [1], the restoration of photon counting imagery can be transformed into a valid estimation of the expectation for photons on each pixel [2]. Photon counting

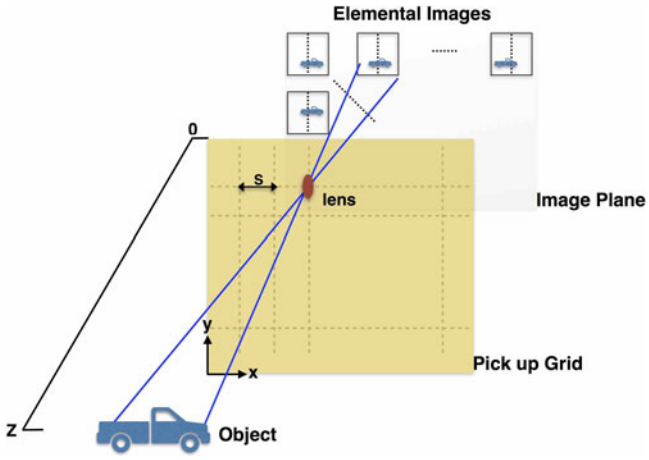

Fig. 1. Photon counting Synthetic Aperture II system.

integral imaging (II) records different perspectives of the scene by a photon counting array [3]. The similarity across the view can contribute to the estimation of Poisson process. Therefore, photon counting II (integral imaging) system, as a three-dimensional (3D) passive imaging system, can be applied to visualize and detect 3D target at low light level [4]–[12].

Based on the Poisson data generated from photon counting II system , a variety of statistical approaches have been introduced to the photon counting 3D reconstruction [4], [8]–[12]. Several authors made efforts to design an estimator to reconstruct more accurate depth slice images, such as the Maximum Likelihood Estimator (MLE) combined with the photon counting process [4], [8] and the Bayesian estimation using the Gamma distribution as a prior distribution [9], [10]. Other efforts chose iterative solutions to solve the reconstruction problem under photon-starved conditions, such as total variation maximum a posteriori expectation maximization (TV MAP-EM) algorithm used to enhance the two-dimensional (2D) photon counting images [11] and penalized maximum likelihood expectation maximization (PMLEM) [12] algorithm with a penalty operator to reflect some prior assumption about the object. By the comparison between these algorithms, prior information plays an important role for the performance of photon counting II reconstruction. However, the chosen prior constrain for unknown scenes may not be the best way to describe object characteristics. Especially for the prior-based PMLEM [12], the penalty operator is controlled by an artificial regularization parameter that causes the instability of the reconstruction performance.

To avoid the search for an optimal prior, in this paper, we propose an adaptive photon counting II reconstruction algorithm. Through the contrast between neighboring pixels, a compound photon counting model for the distribution of the count observation is established. To enhance the visual quality of photon counting images, a variance stabilizing transformation (VST) combined with Block-matching and 3D filtering (BM3D) algorithm [13] is also used. Our proposed algorithm improves the quality of reconstructed depth slice images for the photon counting II system in case of a few photons illumination.

2. Overview of Photon-Counting II Reconstruction

2.1 Photon Counting Synthetic Aperture II System

As an implementation of integral imaging, Synthetic Aperture Integral Imaging (SAII) [14] captures multiple 2D images of the scene by a single camera along x and y directions that are vertical to the optical axis of the cameras lens. As shown in Fig. 1, this series of recorded 2D images, called elemental images, not only contains the irradiance information of the target rays, but also

contains the direction information. Therefore, it is possible to reconstruct the 3D scene from multiple elemental images with different perspectives [15].

To adopt the SAII to photon counting II system, the Poisson process associated with a photon counting detector in the photon-starved conditions should be simulated. For computational simplicity, we use one-dimensional notion only. By introducing the expected number of photons N_p for each elemental image, multi-view photon counting elemental images can be generated from their corresponding gray images as the following equations [8], [11]:

$$\lambda_k^x = \frac{I_k^x}{\sum_{x=1}^{N_x} I_k^x} \tag{1}$$

$$C_k^x | \lambda_k^x \sim Poisson\left(N_p \lambda_k^x\right) \tag{2}$$

where I_k^x is the light intensity at pixel x, N_x is the total number of pixels in each elemental image, λ_k^x is the normalized irradiance at pixel x and C_k^x is the extracted number of photons at pixel x, respectively. The subscript k indicates the location of elemental images.

2.2 Photon Counting II Reconstruction

For the reconstruction of photon counting II system, MLE has been used to reconstruct depth slice images as following [8], [11]:

$$MLE\{\lambda^z\} = \frac{1}{K} \sum_{k=0}^{K-1} \frac{C_k^x}{N_p} \tag{3}$$

where λ^z is the reconstructed depth slice image at depth z. K is the total number of photon counting elemental images superimposed for reconstruction. The reliability of MLE [8] is associated with the expected number of photons for each elemental image and the number of recorded photon counting elemental images. When the number of photons per elemental image or the number of captured elemental images is not enough, it is difficult for MLE to decrease the irradiance estimation error. By further research, the Bayesian framework is applied to the photon counting II reconstruction. The Gamma distribution is used as a prior distribution and then two parameters, namely the shape parameters α and the scale parameters β from the Gamma distribution, are introduced in the final calculation of posterior mean. So, the reconstructed slice images by the Bayesian method can be obtained by [9]:

$$Bayes\{\lambda^z\} = \frac{1}{K} \sum_{k=0}^{K-1} \frac{C_k^x + \alpha_k}{N_p\left(1 + \beta_k\right)} \tag{4}$$

where $\alpha_k = \mu_k^2/\sigma_k^2$, $\beta_k = \mu_k/\sigma_k^2$, μ_k is the mean of λ_k^x, and σ_k^2 is the variance of λ_k^x. However, λ_k^x is what we end to estimate and its statistical information is not provided in advance. Thus, α_k and β_k can only be obtained from the captured photon counting elemental images. In very low illumination environments, photon counting elemental images are extremely sparse. The photons collected by pixels are mostly zero and only a very small number of pixels will detect photons. Therefore, the statistical properties of photon counting elemental images are not sufficient to describe the target details, which results in an improper estimation for α_k and β_k.

3. Proposed Method

3.1 Compound Photon Counting Model

To avoid the prior estimation under Bayesian framework, the MLE based on the compound photon counting model (CMLE) is applied to enhance the visual quality of reconstructed photon-starved objects. For two pixels x and x' in the photon counting elemental images, a compound photon

counting model for them is given according to the additivity of Poisson distribution:

$$C_k^x + C_k^{x'} \sim Poisson\left(N_p\lambda_k^x + N_p\lambda_k^{x'}\right) \tag{5}$$

Here we define a local contrast metric $r_k^x = \lambda_k^{x'}/\lambda_k^x$ to describe the relationship between λ_k^x and $\lambda_k^{x'}$. Then, using a similar MLE reconstruction process [8], the following algorithms can be used for computational reconstruction of photon counting SAII system:

$$L\left(\lambda_k^x\right) = \prod_{k=0}^{K-1} \frac{\left[N_p\lambda_k^x\left(1+r_k^x\right)\right]^{C_k^x+C_k^{x'}} e^{-\left[N_p\lambda_k^x\left(1+r_k^x\right)\right]}}{\left(C_k^x + C_k^{x'}\right)!} \tag{6}$$

$$l\left(\lambda_k^x\right) \propto \sum_{k=0}^{K-1}\left\{\left(C_k^x + C_k^{x'}\right) log\left[N_p\lambda_k^x\left(1+r_k^x\right)\right] - \left[N_p\lambda_k^x\left(1+r_k^x\right)\right]\right\} \tag{7}$$

$$\frac{\partial l\left(\lambda_k^x\right)}{\partial\left(\lambda_k^x\right)} = 0, \qquad \tilde{\lambda_k^x} = \frac{C_k^x + C_k^{x'}}{N_p\left(1+r_k^x\right)} \tag{8}$$

$$CMLE\left\{\lambda^z\right\} = \frac{1}{K}\sum_{k=0}^{K-1}\frac{C_k^x + C_k^{x'}}{N_p\left(1+r_k^x\right)} \tag{9}$$

where L and l are the likelihood function and log-likelihood function, respectively. $\tilde{\lambda_k^x}$ is the estimated elemental images for photon counting 3D reconstruction. Using (6)–(9), the depth slice images can be reconstructed by our proposed method.

In photon counting II system, pixel x is the position where the irradiance of object pixel m, λ^m, falls in the photon counting elemental images. Depending on the corresponding relationship between the image pixel x and the object pixel m, the ratio between $\lambda_k^{x'}$ and λ_k^x can be replaced by the division of $\lambda^{m'}$ and λ^m. Meanwhile, benefited from the multiple realizations of the inhomogeneous Poisson process in the photon counting II system, both $\lambda^{m'}$ and λ^m can be initially estimated as the mean of their corresponding values in the photon counting elemental images. So, r_k^x can be calculated by

$$r_k^x = \frac{\lambda^{m'}}{\lambda^m} = \frac{\sum_{k=0}^{K-1} C_k^{x'}\left(x' + \frac{Sgk}{z_{x'}}\right)}{\sum_{k=0}^{K-1} C_k^x\left(x + \frac{Sgk}{z_x}\right)} \tag{10}$$

where S is the gap for the camera to move on the pick up grid, g is the distance between pick up grid and image plane, z_x is the depth where the object pixel m located at and $z_{x'}$ is the depth where the object pixel m' located at, respectively.

In the proposed photon counting model, the selection of pixel x' plays an important role during the estimation for $\tilde{\lambda_k^x}$ in (8). Depending on the neighborhood centered on pixel x, we select its nearest nonzero pixel as pixel x'. Some kinds of cases should be considered. When C_k^x is nonzero, the nearest nonzero pixel in the neighborhood is itself and then r_k^x equals one. When C_k^x and its neighbor pixels values are all zero, the calculation result of $\tilde{\lambda_k^x}$ is set to zero. When C_k^x is zero but its nearest nonzero pixel is not unique, the pixel that results in the minimum difference between r_k^x and one will be selected.

3.2 Restoration Technique

From the image acquisition model in the photon counting II system, photon counting elemental images suffer the low counts of photons in the photon-starved scenes and Poisson noise becomes the dominant noise. To enhance the visual quality of the estimated elemental images $\tilde{\lambda_k^x}$ from (8), the restoration technique named VST combined with BM3D algorithm [13] is introduced to denoise these elemental images. The algorithm flow is as follows:

1) Forward VST

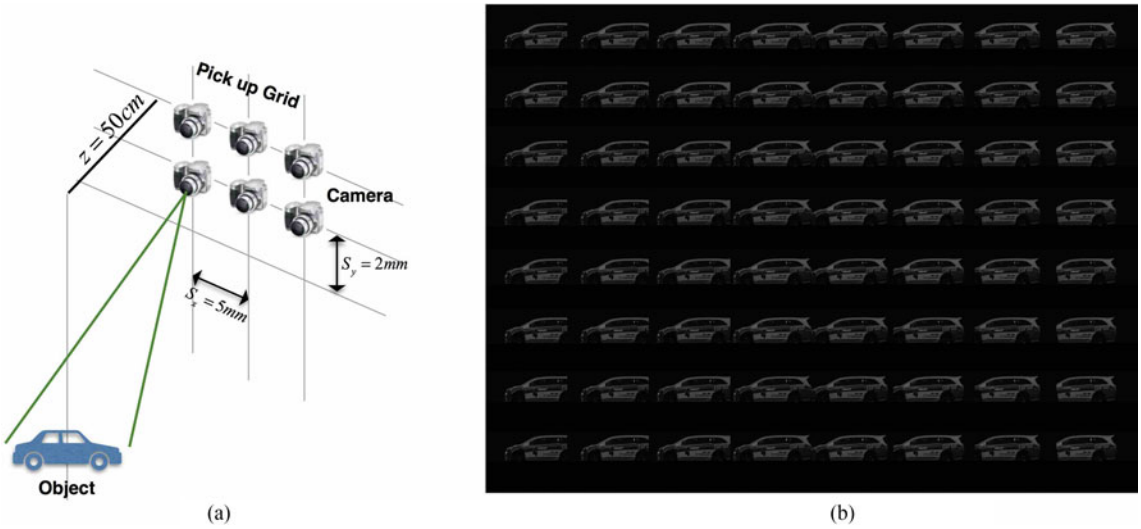

Fig. 2. (a) Experiment setup; (b) 8 × 8 gray elemental images.

Let r be the noisy image modeled as independent realizations of a Poisson process with parameter y. According to the archetypal VST framework, the Anscombe forward transformation a is applied to standard the noisy image [16]:

$$a(r) = 2\sqrt{r + 3/8} \tag{11}$$

2) BM3D
The transformed image $a(r)$ can be treated as corrupted by additive white Gaussian noise (AWGN) with unit variance. Thus, it can be denoised by any Gaussian denoising algorithms.Here, the BM3D filter Φ is used [17]:

$$\Phi[a(r)] = E\{a(r)|y\} \tag{12}$$

3) Exact unbiased inverse
The operator I_a is used to return the denoised image to the original range of r [13]:

$$I_a : E\{a(r)|y\} \mapsto E\{r|y\} = y \tag{13}$$

4. Experiments and Results

Experiments to verify proposed statistical approach for photon-limited objects are presented as shown in Fig. 2(a). Under normal illumination conditions, a single camera with focal length 35 mm and 658(H) × 492 (V) pixels is used. The moving gaps between image sensing positions in x-y directions are 5 mm and 2 mm, respectively. The 3D object is located at $z = 50$ cm away from the center of the pickup grid. Using this experimental setup, 8 × 8 gray elemental images are captured as shown in Fig. 2(b).

Photon counting elemental images can be generated from the grayscale elemental images by using (1) and (2). We set $N_p = 1000$ and so the ratio between the expected number of photons and image pixels in the elemental image [658(H) × 492 (V)] is approximately 0.3%. According to the photon counting elemental image ($N_p = 1000$) generated from the gray elemental image in Fig. 3(a), Fig. 3(b) and (c) illustrate the estimated elemental image using MLE and using CMLE, respectively. Apparently, the estimated elemental image with CMLE visuals the objects better than that with MLE. To further enhance the quality of estimated elemental images, as depicted in Fig. 3(d) and (e), VST combined with BM3D algorithm (VST+BM3D) [see (11)–(13)] is used to restore the images in Fig. 3(b) and (c), respectively.

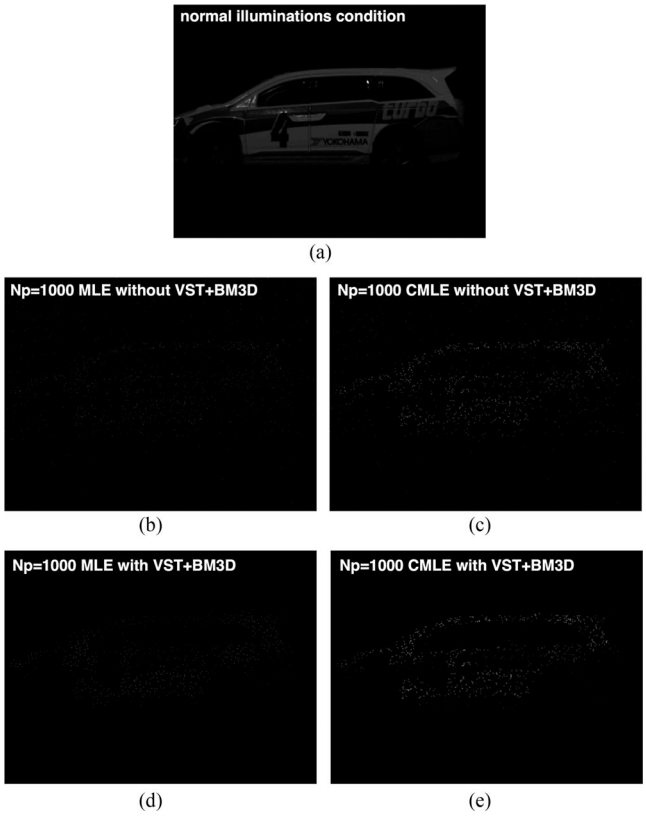

Fig. 3. Estimated elemental images ($N_p = 1000$): (a) under normal illumination conditions; (b) MLE without VST+BM3D algorithm; (c) CMLE without VST+BM3D algorithm; (d) MLE with VST+BM3D algorithm; (e) CMLE with VST+BM3D algorithm.

Fig. 4 shows the reconstructed depth slice images at depth $z = 50$ cm for the photon counting imaging system ($N_p = 1000$) with SAII. Fig. 4(a) is the reconstructed image under normal illumination conditions as the reference image. In Fig. 4(b), MLE without VST+BM3D algorithm is used to reconstruct depth slice images. On the other hand, proposed CMLE without VST+BM3D algorithm is applied to reconstruct depth slice images in Fig. 4(c). It can be seen that our proposed CMLE algorithm yields better visual reconstruction than MLE algorithm.

Furthermore, VST+BM3D algorithm is applied to Fig. 4(b) and (c) for investigating its contributions in severe photon-starved conditions qualitatively. The reconstruction results of MLE and CMLE with VST+BM3D algorithm both have better visual quality than those without VST+BM3D algorithm as shown in Fig. 4(d) and (e).

To confirm the generality of this result, we add more experimental results. Fig. 5(a) shows the gray elemental image under regular illumination conditions and Fig. 5(b) is the photon counting elemental image with average photon count of 0.3% per pixel, respectively. As shown in Fig. 5(c), it is difficult to recognize the object from the reconstructed image using the conventional MLE without VST+BM3D algorithm. However, proposed CMLE with VST+BM3D algorithm gives better result as shown in Fig. 5(d). The other experimental result under average photon count of 0.3% per pixel is shown in Fig. 6. Compared to conventional MLE, the better reconstruction result by using our proposed method is proved again.

By varying the value of N_p to generate different photon counting integral images from the gray elemental images in Fig. 2(b), Fig. 7 shows the change of peak signal to noise ratio (PSNR) as a function of N_p for comparison between our proposed method and MLE method. The randomness of photon counting process causes a nonlinear growth in PSNR. In the case of MLE

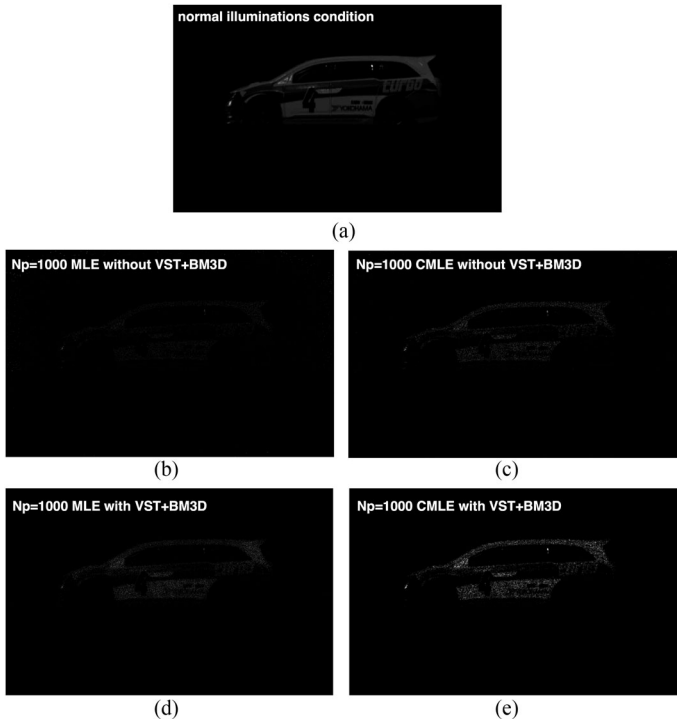

Fig. 4. Reconstruction results: (a) under normal illumination conditions; (b) MLE without VST+BM3D algorithm; (c) CMLE without VST+BM3D algorithm; (d) MLE with VST+BM3D algorithm; (e) CMLE with VST+BM3D algorithm.

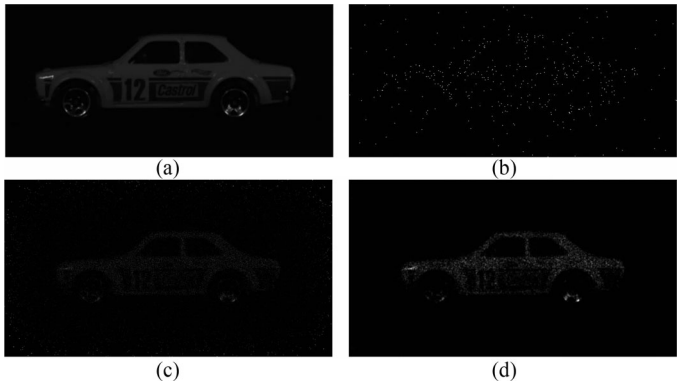

Fig. 5. Experimental results: (a) elemental image under normal illumination conditions; (b) photon counting elemental image; (c) reconstruction result using MLE without VST+BM3D algorithm; (d) reconstruction result using CMLE with VST+BM3D algorithm.

without VST+BM3D algorithm, the PSNR varies very slightly with the increase of N_p. Whether or not it contains the VST+BM3D algorithm, our proposed CMLE method always has a higher PSNR than MLE and the advantage is more obvious along with the increasing of N_p, that is, the performance of proposed method is not limited as we increase the number of photons expected in the scene. When comparing the reconstructed images with $N_p = 1000$ [see Fig. 4], the PSNR of MLE without VST+BM3D algorithm is 23.7556 dB and the PSNR of CMLE with VST+BM3D

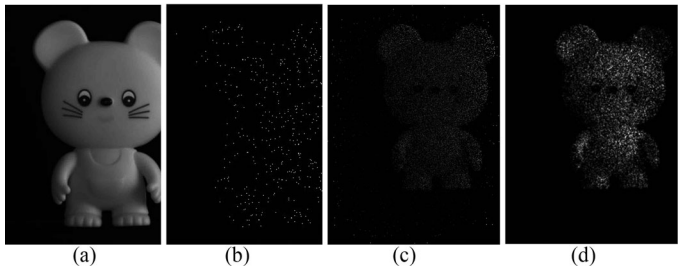

Fig. 6. Experimental results: (a) elemental image under normal illumination conditions; (b) photon counting elemental image; (c) reconstruction result using MLE without VST+BM3D algorithm; (d) reconstruction result using CMLE with VST+BM3D algorithm.

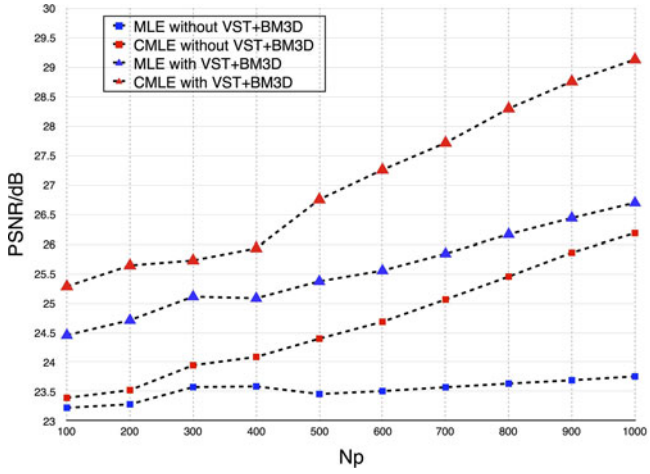

Fig. 7. PSNR of reconstruction results for photon counting imaging using SAII.

algorithm is 29.129 dB. Our proposed method has 5.4 dB higher PSNR than the conventional MLE method.

5. Conclusions

In conclusion, we propose an adaptive parametric MLE method to reconstruct the scene by photon counting II system. Assuming a compound photon counting model for the number of photons, a pixel-dependent adaptive parameter is introduced to the solution of MLE. Restoration technique (VST+BM3D algorithm) is used to enhance the visual quality of photon counting elemental images. We have calculated the PSNR to compare with the conventional MLE using a Poisson model. It is shown that our proposed parametric MLE with VST+BM3D algorithm yields better reconstruction than the conventional MLE algorithms, both visually and in terms of PSNR.

References

[1] J. W. Goodman, *Statistical Optics*. Hoboken, NJ, USA: Wiley, 2015.
[2] M. Bertero, P. Boccacci, G. Desider, and G. Vicidomini, "Image deblurring with Poisson data: From cells to galaxies," *Inverse Probl.*, vol. 25, 2009, Art. no. 123006.
[3] S. Yeom, B. Javidi, and E. Watson, "Three-dimensional distortion-tolerant object recognition using photon-counting integral imaging," *Opt. Exp.*, vol. 15, pp. 1513–1533, 2007.
[4] I. Moon and B. Javidi, "Three dimensional imaging and recognition using truncated photon counting model and parametric maximum likelihood estimator," *Opt. Exp.*, vol. 17, pp. 15709–15715, 2009.

[5] I. Moon and B. Javidi, "Three-dimensional recognition of photon-starved events using computational integral imaging and statistical sampling," *Opt. Letters*, vol. 34, pp. 731–733, 2009.
[6] M. DaneshPanah, B. Javidi, and E. A. Watson, "Three dimensional object recognition with photon counting imagery in the presence of noise," *Opt. Exp.*, vol. 18, pp. 26450–26460, 2010.
[7] M. Cho, A. Mahalanobis, and B. Javidi, "3D passive photon counting automatic target recognition using advanced correlation filters," *Opt. Lett.*, vol. 36, pp. 861–863, 2011.
[8] B. Tavakoli, B. Javidi, and E. Watson, "Three dimensional visualization by photon counting computational integral imaging," *J. Display Technol.*, vol. 16, pp. 4426–4436, 2008.
[9] J. Jung, M. Cho, D. K. Dey, and B. Javidi, "Three-dimensional photon counting integral imaging using Bayesian estimation," *Opt. Lett.*, vol. 35, pp. 1825–1827, 2010.
[10] M. Cho, "Three-dimensional color photon counting microscopy using Bayesian estimation with adaptive priori information," *Chin. Opt. Lett.*, vol. 13, 2015, Art. no. 070301.
[11] M. Cho and B. Javidi, "Three-dimensional photon counting axially distributed image sensing," *J. Display Technol.*, vol. 9, no. 1, pp. 56–62, Jan. 2013.
[12] D. Aloni, A. Stern, and B. Javidi, "Three-dimensional photon counting integral imaging reconstruction using penalized maximum likelihood expectation maximization," *Opt. Exp.*, vol. 19, pp. 19681–19687, 2011.
[13] M. Makitalo and A. Foi, "Optimal inversion of the Anscombe transformation in low-count Poisson image denoising," *IEEE Trans. Image Process.*, vol. 20, no. 1, pp. 99–109, Jan. 2011.
[14] J.-S. Jang and B. Javidi, "Three-dimensional synthetic aperture integral imaging," *Opt. Lett.*, vol. 27, pp. 1144–1146, 2002.
[15] S.-H. Hong, J.-S. Jang, and B. Javidi, "Three-dimensional volumetric object reconstruction using computational integral imaging," *Opt. Exp.*, vol. 12, pp. 483–491, 2004.
[16] F. J. Anscombe, "The transformation of Poisson, binomial and negative-binomial data," *Biometrika*, vol. 35, pp. 246–254, 1948.
[17] K. Dabov, A. Foi, V. Katkovnik, and K. Egiazarian, "Image denoising by sparse 3-D transform-domain collaborative filtering," *IEEE Trans. Image Process.*, vol. 16, no. 8, pp. 2080–2095, Aug. 2007.